

Spring Roll Dielectric Elastomer Actuators for a Portable Force Feedback Glove

Rui Zhang^a, Patrick Lochmatter^a, Andreas Kunz^b and Gabor Kovacs^a

^aLaboratory for Materials and Engineering,
Swiss Federal Laboratories for Materials Testing and Research,
8600 Dubendorf, Switzerland

^bInstitute of Machine Tools and Manufacturing,
Swiss Federal Institute of Technology,
8092 Zurich, Switzerland

ABSTRACT

Miniature spring roll dielectric elastomer actuators for a novel kinematic-free force feedback concept were manufactured and experimentally characterized. The actuators exhibited a maximum blocking force of 7.2 *N* and a displacement of 5 *mm*. The theoretical considerations based on the material's incompressibility were discussed in order to estimate the actuator behavior under blocked-strain activation and free-strain activation. One prototype was built for the demonstration of the proposed force feedback concept.

Keywords: Electroactive polymer, dielectric elastomer, spring roll actuator, force feedback, virtual reality

1. INTRODUCTION

Virtual reality can be traced to about fifty years ago when Morton Heilig, a cinematographer, began designing the first multisensory virtual experiences. In order to enable spectators to be fully immersed in a film scene, he developed a "Sensorama Simulator", which combined projected film, audio, vibration, wind and even odors.¹ Nowadays, after an interesting and complex history,² virtual reality, a real-time and multi-sensorial human-environment interface, is used in wide range of applications.³⁻⁶

However, a lack of realistic touch sensation is still one of the drawbacks, which prevents virtual reality from reaching its full potential. Particularly, force feedback devices (FFD) that allow users to intuitively grasp and manipulate virtual objects have been demanded for many applications.⁷

Such devices can generally be divided into ground-based and body-based types in respect of their location. The former is fixed to its environments such as desk, ceiling, wall or floor, while the latter is attached to a part of human body like shoulder, arm or hand. Ground-based devices based on PHANTOM or Delta^{6, 8-10} can provide quite strong forces against the user's fingers. However, implicit friction and backlash, limited workspace and the absence of portability are their drawbacks. On the opposite, body-based devices^{3, 11-14} are portable and provide therefore larger workspace in virtual environment. However, this portability is achieved at the sacrifice of their ergonomics, since the user has to carry the device as a whole or part of it.

Force transmission mechanisms like exoskeleton plus cable-pulley structures can often be seen in portable devices.^{3, 11, 13, 14} These are bulky, heavy, and mechanically complex systems with high internal frictions and high inertia. Furthermore, these devices exhibit poor transparency¹⁰ and dynamic performances. The adjustment of such mechanisms to fit different sizes of hands is time-consuming, and may cause errors in position sensing. Furthermore, the attachments of such a structure on the hand introduce unwanted forces, which may strongly disturb the user.

One way of avoiding such force transmission structures is to apply the actuators' forces directly on the contact areas*. The actuators can be located either on the palm side or on the dorsal side of the hand. In both cases,

Send correspondence to Rui Zhang: E-mail: rui.zhang@empa.ch, Telephone: +41 (0)44 823 4625

*in this paper this is denoted by "kinematic-free" since no extra force transmission structure that causes a complex kinematic structure is required. Some authors defined this as "direct driven".¹⁴

actuators with high elongation and force, fast response, high energy density, sufficient safety, non-noise operating, simple control law, favorable energy source and price are required.

In our previous paper, we discussed the feasibilities of using shape memory alloys, piezo materials, electro/magneto rheological fluids or electroactive polymers (EAP) as driving actuators for portable and kinematic-free force feedback devices.¹⁵ Dielectric elastomers (DE), a subgroup of EAP, showed a good overall performance and was chosen as candidate actuation technology.¹⁵⁻¹⁷

We presented a conceptual force feedback glove with integrated tendon-like actuators on the fingers' dorsal side.^{15,16} The vision is to have a force feedback glove that is as compact and comfortable as a normal cotton glove for the user. The tendon-like actuators provide forces on the fingertips by pulling them backwards, so that a kinematic-free fashion could be achieved. An elementary planar DE actuator for this concept exhibited a displacement of 7.5 mm and a contractile force of 0.7 N under a pre-stretching force of 2 N. The challenge for such planar DE actuators is the design of a housing, which must hold biaxial pre-strains in the film (VHB 4910 3M) while allowing one degree of freedom for the active deformation. The bulky and relatively heavy housing compared to the active material made the actuator far away from the practical application.

Pei et al^{18,19} have developed multi-DOF spring roll DE actuators by wrapping pre-stretched DE films around a spiral spring core. The core maintained pre-strains in the dielectric film and enhanced the ratio of the effective film's mass to the passive material's mass. However, having low buckling strength, the spring roll DE actuator allows limited compressive forces.

In this study, we briefly introduce a kinematic-free force feedback concept and the requirements on a DE actuator in Sect. 2. In Sect. 3, the manufacturing, its working principle, some theoretical considerations on diverse activation states and the general performance of a miniature spring roll DE actuator are discussed. Subsequently, the experimental measurements and results are given in Sect. 4. One demonstrator is shortly presented in Sect. 5.

2. CONCEPT FOR A NEW PORTABLE FORCE FEEDBACK DEVICE

A force feedback device has two major functions: (1) allowing free motions of the user's fingers if there is no interaction between the user's hand and a virtual object and (2) providing the fingertips with a specific force when an interaction occurs (see Fig. 1(a) and 1(b)). As shown in Fig. 1(c), a novel concept in kinematic-free fashions was developed.¹⁷ By connecting actuators between the fingers, there is no unnatural grounding forces of the actuators on the user's hand. However, simulation metaphors are limited to only object-grasping simulations.

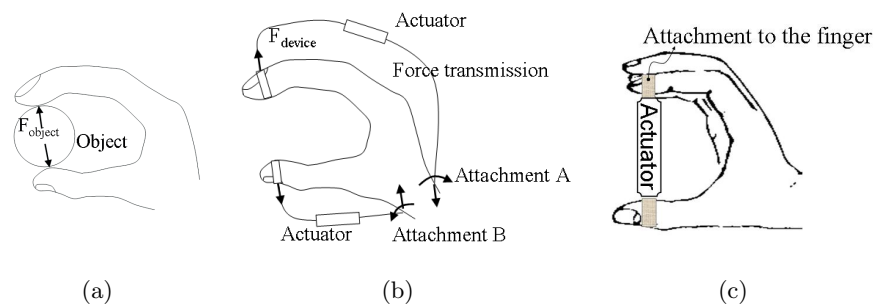


Figure 1. External resulting forces from the object act against the finger flexion in precision grasping (a), the contact model of the finger-device grasping (b), and the selected concept for kinematic-free force feedback device.

In Tab. 1 requirements on a spring roll DE actuator are defined according to the proposed force feedback concept.

Table 1. Requirements on a spring roll DE actuator for the kinematic-free force feedback concept.

Requirement	Specification
Sustainable force	up to 7 N @ 8-30 Hz ^{20, 21}
Max. force	up to 45 N ²²
Elongation	40% @ 1-5 Hz ²¹
Weight	10 g per actuator
Dimensions	$\varnothing=15\text{ mm}$, $L=40\text{ mm}$

3. MINIATURE SPRING ROLL DIELECTRIC ELASTOMER ACTUATORS

Basically, a DE actuator is a compliant capacitor. A thin elastomeric film is sandwiched between two compliant electrodes. Under activation with a high DC voltage (kV), the electrostatic pressure squeezes the elastomer film in thickness and thus, the incompressible film expands in planar directions. By properly configuring the DE actuator, the three-dimensional deformation of the film can be transferred into axial,^{23, 24} bending and radial motion.

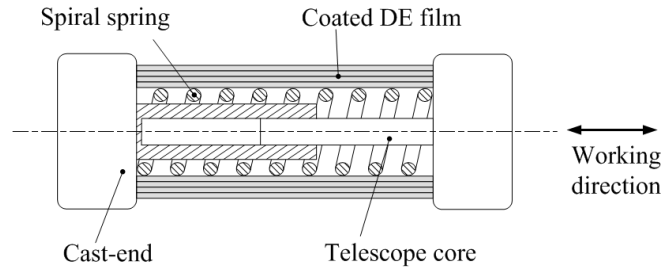


Figure 2. Structure of the spring roll DE actuator with telescope core inside the spiral spring

As shown in Fig. 2, the spring roll DE actuator consists of a biaxially pre-stretched DE film, which is wrapped around a fully compressed spiral spring. In order to transmit the strong expansion forces of the spring to the dielectric film, the spring and the film are casted up on both ends. By implementing a mechanical telescope guidance the actuator is able to execute linear movements and to hold axial compressive loads introduced by the fingers. The miniature spring roll DE actuators have been made at Empa Dubendorf based on a half-automated manufacturing process.

3.1. Working Principle

The characteristics of the spring as well as the passive/activated DE film are plotted qualitatively in a force-displacement diagram in Fig. 4. By activating or deactivating the actuator, and setting the working boundary condition, the following four states can be achieved:

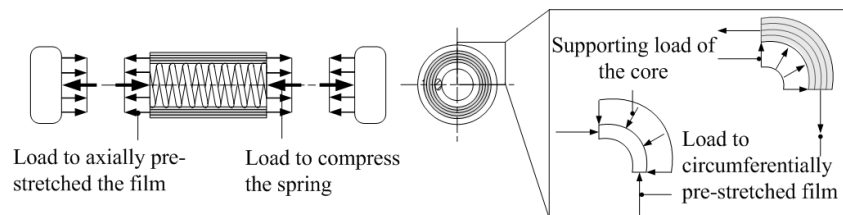


Figure 3. Passive equilibrium of axial/radial/circumferential loads in the spring roll DE actuator.

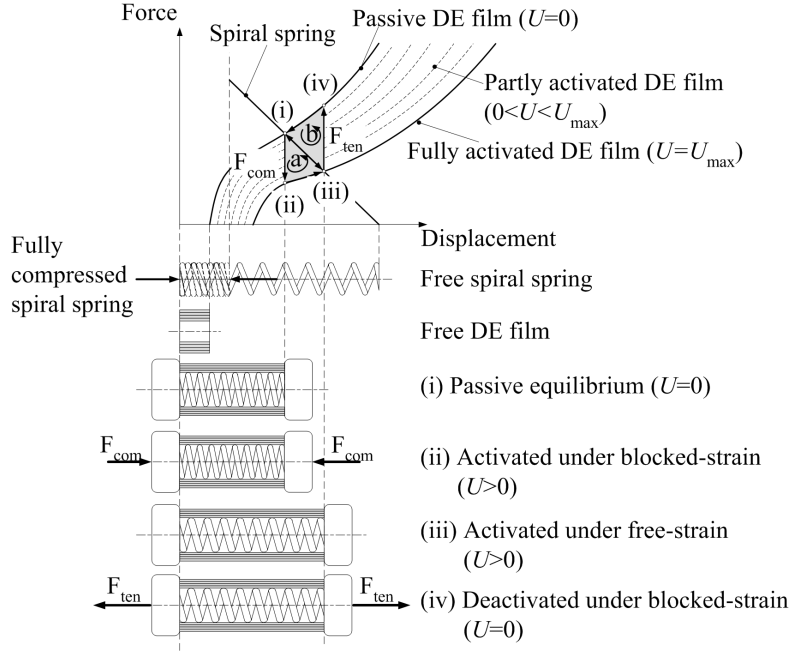


Figure 4. Four states of the spring roll DE actuator.

- (i) *Passive equilibrium:* A passive spring roll DE actuator is in a force equilibrium. In axial direction the DE film is pre-stretched by the compressed spiral spring. In radial direction the circumferential loads of the pre-stretched DE film are supported by the spring core (details refer to Fig. 3).
- (ii) *Activated under blocked-strain:* Under electrical activation from the passive equilibrium state (i) the film relaxes and releases the compressed spring. An external compressive force F_{com} (e.g. from the finger if used in the proposed FFD concept) is required to prevent the expansion of the spring in order to maintain the length of the actuator. This force is denoted as compressive blocking force.
- (iii) *Activated under free-strain:* Under electrical activation from the passive equilibrium state (i) the film relaxes and thus, the spring expands until the forces from spring and DE film are balanced in a new axial equilibrium.
- (iv) *Deactivated under blocked-strain:* When fixing the length of the actuator in the activated state (iii) and subsequently deactivating the actuator, an external tensile force F_{ten} is required to prevent the actuator from contracting. This force is denoted as tensile blocking force.

3.2. Considerations on the Blocked-strain Activation

For a blocked-strain activation of the spring roll DE actuator from passive equilibrium state (i) the compressive force F_{com} as a function of the activation voltage U is estimated by taking into account that the used film (VHB4910, 3M) is incompressible.

During manufacturing of the spring roll DE actuator the film is initially pre-stretched by planar stresses $\sigma_x^{(i)}$ and $\sigma_y^{(i)}$ to planar stretch ratios $\lambda_x^{(i)}$ and $\lambda_y^{(i)}$ in state (i) (shown in Fig. 5). Based on the boundary conditions (in x: $\sigma_x = \sigma_x^{(i)}$, $\lambda_x = \lambda_x^{(i)}$; in y: $\sigma_y = \sigma_y^{(i)}$, $\lambda_y = \lambda_y^{(i)}$; in z: $\sigma_z = 0$, $\lambda_z = \lambda_z^{(i)}$) the Cauchy-stresses²⁵ for the pre-strain state (i) are thus given by:

$$x : \sigma_x^{(i)} = \lambda_x^{(i)} \frac{\partial w}{\partial \lambda_x} \Big|^{(i)} - p_h^{(i)}$$

$$\begin{aligned}
y : \sigma_y^{(i)} &= \lambda_y^{(i)} \frac{\partial w}{\partial \lambda_y} \Big|^{(i)} - p_h^{(i)} \\
z : 0 &= \lambda_z^{(i)} \frac{\partial w}{\partial \lambda_z} \Big|^{(i)} - p_h^{(i)}
\end{aligned} \tag{1}$$

Thereby, w is the strain energy potential of the film, $p_h^{(i)}$ is the hydrostatic pressure in the film, and $\lambda_j^{(i)}$ is the film's stretch ratio in directions $j=x,y,z$ in state (i) .

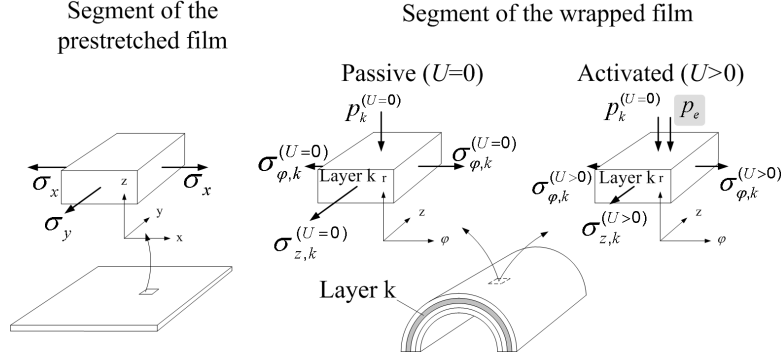


Figure 5. Load consideration in the spring roll DE actuator and the electromechanical coupling under blocked-strain activation.

The film is then wrapped around the spiral spring core (e.g. axis of spiral spring in y direction). Thus, the film's coordinates change from planar to cylindrical according to $x \rightarrow \varphi$, $y \rightarrow z$, $z \rightarrow r$. For the present investigation the wrapped film must axially countervail the compressed spring so that the pre-strain state of the film (i) corresponds to the state in passive equilibrium. Assuming that the thickness of the pre-stretched film $d^{(i)} = d^{(0)} / \lambda_x^{(i)} \lambda_y^{(i)}$ is by far smaller than the core radius R ($d^{(i)} \ll R$) the Cauchy-stresses can be applied to the wrapped film as well. Furthermore, the wrapped film is replaced by a stack of N concentric cylindrical film layers. For the general layer k (boundary conditions in r : $\sigma_r = -p_k^{(U=0)}$, $\lambda_r = \lambda_z^{(i)}$; in φ : $\sigma_\varphi = \sigma_{\varphi,k}^{(U=0)}$, $\lambda_\varphi = \lambda_x^{(i)}$; in z : $\sigma_z = \sigma_{z,k}^{(U=0)}$, $\lambda_z = \lambda_y^{(i)}$) the Cauchy-stresses in the passive state ($U = 0$) are thus given by:

$$\begin{aligned}
r : -p_k^{(U=0)} &= \lambda_z^{(i)} \frac{\partial w}{\partial \lambda_z} \Big|^{(i)} - p_h^{(U=0)} \\
\varphi : \sigma_{\varphi,k}^{(U=0)} &= \lambda_x^{(i)} \frac{\partial w}{\partial \lambda_x} \Big|^{(i)} - p_h^{(U=0)} \\
z : \sigma_{z,k}^{(U=0)} &= \lambda_y^{(i)} \frac{\partial w}{\partial \lambda_y} \Big|^{(i)} - p_h^{(U=0)}
\end{aligned} \tag{2}$$

Under blocked-strain activation the geometry of the wrapped DE film is retained since the actuator core is rigid and the actuator length is fixed. Thus, for the Cauchy-stresses in the activated state ($U > 0$) the equivalent electrostatic pressure p_e ²⁶

$$p_e = \varepsilon_0 \varepsilon_r \left(\frac{U}{d^{(i)}} \right)^2 \tag{3}$$

is to be superimposed in radial direction ($\sigma_r = -p_k^{(U>0)} = -p_k^{(U=0)} - p_e$). The active Cauchy-stresses are then given by:

$$\begin{aligned}
r : -p_k^{(U>0)} &= \lambda_z^{(i)} \frac{\partial w}{\partial \lambda_z} \Big|^{(i)} - p_h^{(U>0)} \\
\varphi : \sigma_{\varphi,k}^{(U>0)} &= \lambda_x^{(i)} \frac{\partial w}{\partial \lambda_x} \Big|^{(i)} - p_h^{(U>0)} \\
z : \sigma_{z,k}^{(U>0)} &= \lambda_y^{(i)} \frac{\partial w}{\partial \lambda_y} \Big|^{(i)} - p_h^{(U>0)}
\end{aligned} \tag{4}$$

By implementing Eqs. (1) into Eqs. (2) for the passive Cauchy-stresses ($U=0$), and into Eqs. (4) for the activated Cauchy-stresses ($U>0$), the resulting compressive force F_{com} in axial direction under blocked-strain activation can be derived:

$$\begin{aligned}
 F_{com} &= \left(F_{spring}^{(i)} - F_{film,z}^{(U>0)} \right) - \left(F_{spring}^{(i)} - F_{film,z}^{(U=0)} \right) \\
 &= \sum_{k=1}^N A_{z,k}^{(i)} \left(\underbrace{\sigma_{z,k}^{(U=0)} - \sigma_{z,k}^{(U>0)}}_{p_e} \right) \\
 &= A_{film,z}^{(i)} p_e = A_{film,z}^{(i)} \varepsilon_0 \varepsilon_r \left(\frac{U}{d^{(i)}} \right)^2 \tag{5}
 \end{aligned}$$

Thereby, $F_{spring}^{(i)}$ is the spring force and $A_{film,z}^{(i)}$ is the axial cross-section area of the DE film in the pre-stretched equilibrium state (i). Obviously, the change in radial pressure under activation is directly transmitted via the hydrostatic pressure into the axial direction. Thus, a quadratic increase in axial compressive force as a function of the voltage is expected.

3.3. Considerations on the Free-strain Activation

Under free-strain activation of the spring roll DE actuator the film elongates in axial direction due to the radial compression by the electrostatic pressure. For the detailed theoretical investigation of the actuator under free-strain activation a material model for the dielectric film has to be applied. Based on the incompressibility condition of the dielectric film, however, some basic considerations of the spring roll DE actuator under passive or active axial straining can be achieved.

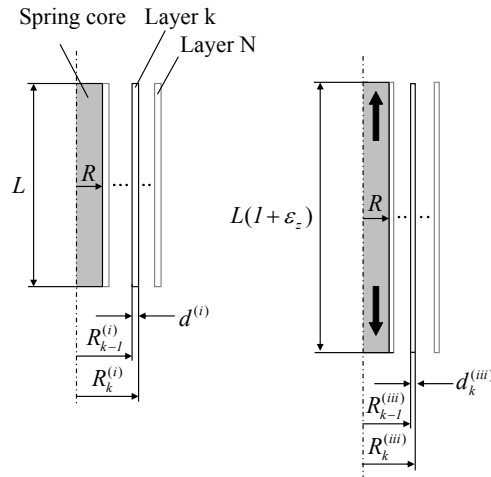


Figure 6. Spring roll DE actuator in the passive equilibrium state (left) and axially elongated state (right).

The film is biaxially pre-stretched with stretch ratios $\lambda_x^{(i)}$ and $\lambda_y^{(i)}$. The film thickness is then calculated by $d^{(i)} = d^{(0)} / \lambda_x^{(i)} \lambda_y^{(i)}$. We consider that the spring roll DE actuator consists of a rigid core with radius R and length L on which $k = 1, 2, \dots, N$ cylinder shells of pre-stretched dielectric film with thickness $d^{(i)}$ are concentrically stacked on top of each other (shown in Fig. 6 left). The inner radius of the film layer k is given by $R_{k-1}^{(i)}$ and the outer radius by $R_k^{(i)}$, respectively.

When the actuator is elongated axially by ε_z ($L \rightarrow L(1 + \varepsilon_z)$) to the state (iii) in Fig. 4 the film layers are axially elongated to the same degree (shown in Fig. 6 right). The radius R of the spiral spring in the core is assumed

to be maintained. Applying that the volume of layer k in state (i) and (iii) must be equal (incompressibility condition) the following relation can be found for the standardized thickness of layer k in the strained state (iii) :

$$\frac{d_k^{(iii)}}{d^{(i)}} = \frac{R_k^{(iii)} - R_{k-1}^{(iii)}}{d^{(i)}} = \sqrt{\frac{2\left(\frac{R}{d^{(i)}}\right) + 2k - 1}{1 + \varepsilon_z} + \left(\frac{R_{k-1}^{(iii)}}{d^{(i)}}\right)^2} - \left(\frac{R_{k-1}^{(iii)}}{d^{(i)}}\right) \quad (6)$$

This recursive equation is evaluated for the spring roll DE actuator developed in this study. Given $R=3.5 \times 10^{-3} m$, $d^{(0)}=10^{-3} m$, $\lambda_x^{(i)} \times \lambda_y^{(i)}=6.5 \times 3$, the resulting standardized film thicknesses for layer $k = 1, 2, \dots, 100$ are plotted in Fig. 7 for axial strain levels $\varepsilon_z=10\%$, 20% , 30% and 40% .

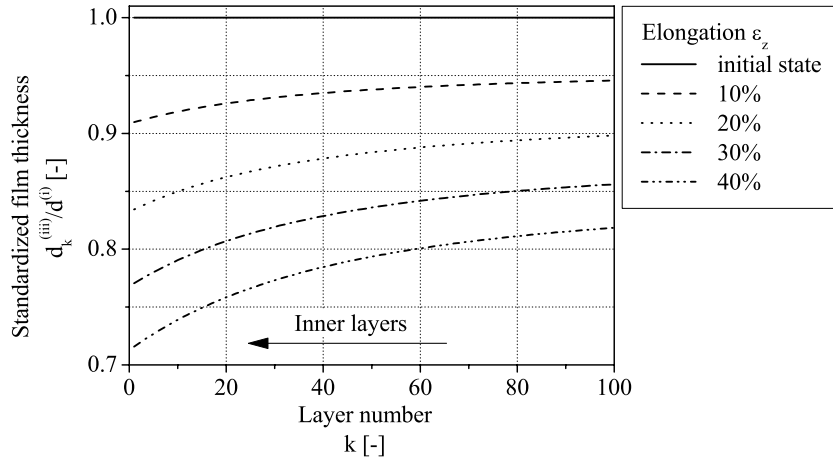


Figure 7. Thickness distribution of the spring roll DE actuator under free-strain activation.

Obviously, under axial elongation the thickness of the inner film layers decreases significantly stronger compared to the outer layers. The effect becomes more dramatic for stronger axial elongations. Under electrical activation this leads to an accumulation of electrical charges in the domain of the thinner layers and thus, the electrical field will be increased in the inner layers. Therefore, under free-strain activation an electrical breakdown tends to occur in the inner layers of the spring roll DE actuators already at lower activation voltages.

3.4. General Performance of Spring Roll DE Actuators

As major performance parameters for DE actuators the overall electromechanical efficiency and the specific energy density are discussed. The overall electromechanical efficiency η is given by the ratio between electrical input energy W_{elec} and mechanical work output W_{mech} per activation cycle:

$$\eta = \frac{W_{elec}}{W_{mech}}, \quad (7)$$

The specific energy density w_V on the other hand is defined as the mechanical work output W_{mech} per cycle and actuator volume V :

$$w_V = \frac{W_{mech}}{V}, \quad (8)$$

Considering the working states of spring roll DE actuators in Fig. 4, two potential work cycles may be:

- (a) $(i) \rightarrow (ii)$ blocked-strain activation, $(ii) \rightarrow (iii)$ elongation against a continuously decreasing compressive load and $(iii) \rightarrow (i)$ free-strain deactivation.

- (b) $(i) \rightarrow (iii)$ free-strain activation, $(iii) \rightarrow (iv)$ blocked-strain deactivation, and $(iv) \rightarrow (i)$ contraction against a continuously decreasing tensile load.

Thereby, the area enclosed by the counter clockwise work cycle curves in the force-displacement diagram corresponds to the mechanical work output per cycle W_{mech} . Obviously, the optimal work output is reached when the two cycles (a) and (b) are combined to the process $(i) \rightarrow (ii) \rightarrow (iii) \rightarrow (iv)$.

Regarding above loops, the source only provides electrical energy during the activation phases $(i) \rightarrow (ii)$ or $(i) \rightarrow (iii)$ according to:

$$W_{elec} = \int U \cdot I dt \quad (9)$$

Thereby, U corresponds to the voltage provided by the source and I is the current in the actuator circuit. Note that the deactivation of the DE actuator is accomplished by short-circuiting the electrodes. Thus, the electrical field energy plus part of the deformation energy (depending on the actuator's boundary conditions) is dissipated as heat in the resistor of the actuator circuit.

3.5. Application of the Spring Roll DE Actuator in FFD

For FFD applications, free-strain, blocked-strain (for compressive or tensile blocking forces), and a combination of both are often used boundary conditions for the simulation of free-motion, hard objects, or diverse elastic objects respectively. This means that the whole shaded area in Fig. 4 enables the actuator to be well used in FFD applications.

It has to be pointed out that the maximum blocking forces decrease as the displacement increases. The maximum blocking forces or free elongation only allows the actuator to simulate hard or soft tissues. To cover wide simulation metaphors (i.e. to present diverse object stiffness), the force-displacement curve of the actuator has to cover the shaded area in Fig. 8, where amplitude of the sustainable force and free motion displacement are defined by human touch perception capability, and features of object-grasping.

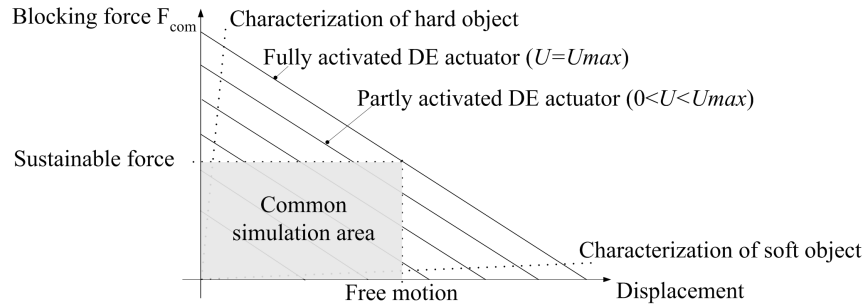


Figure 8. Qualitative force-displacement behavior of the actuator and its application in FFDs.

4. EXPERIMENTAL CHARACTERIZATION

In order to determine the force-displacement behavior as a function of the activation voltage of the spring roll DE actuators, *passive uniaxial tensile tests* and *isometric tests under activation* were performed.

4.1. Measurement Setup

As shown in Fig. 9, we attached one side of the actuator to the grounded-frame, and the other side to a force sensor (HBM U2B), which was mounted on a pneumatic cylinder (BRAMATI²⁷). The displacement of the actuator was measured by the laser sensor (OADM20I6460/S1 4F). The measurement signals were controlled by LabView via an optoelectronic coupler and a data acquisition card (BNC 2090).

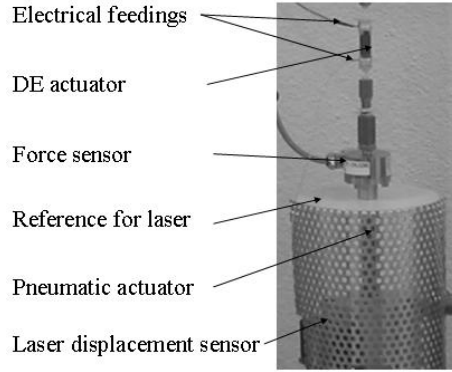


Figure 9. Setup of the passive tensile test and isometric tests under activation.

4.2. Measurements

In the *passive uniaxial tensile tests*, the actuator was stretched by the pneumatic cylinder from its free-standing length to 10 mm with an elongation rate of 2 mm/min. Thereby, the tensile force of the actuator was measured.

During the *isometric test under activation*, two control signals were given by LabView: a DC activation voltage (provided by PS350, Stanford Research Systems) for the actuator, and a displacement control for the pneumatic cylinder. First, the actuator was kept in its passive equilibrium length. A DC activation voltage was linearly increased from 0 to 3.5 kV within 90 s. The compressive blocking force of the actuator was measured. Second, the actuator was stretched to 1 mm with an elongation rate of 2 mm/min. While keeping this position the activation voltage was raised from 0 to 3.5 kV, and the axial force was measured. This procedure was repeated by stretching the actuator each time 1 mm further, until a displacement of 8-10 mm was reached.

4.3. Results

We tested 30 spring roll DE actuators in different groups with slight differences in constructions and aging (due to the viscosity of the elastomer film). All results showed a quasi-linear force-displacement behavior.

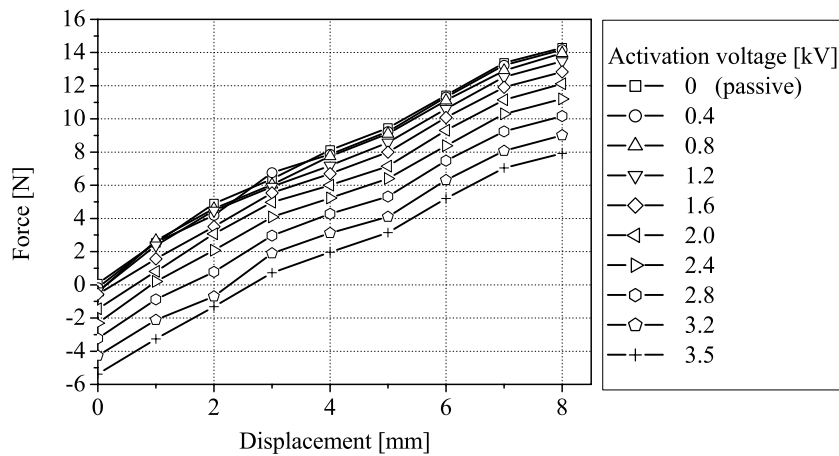


Figure 10. Force-displacement behavior of the DE actuator under different activation voltages.

As shown in Fig. 10, the measured force decreased as the linearly increasing voltage was applied for all initial pre-strains in the range of 0-8 mm. As expected in Sect. 3.5, Fig. 10 shows that a maximum compressive

blocking force of 5.5 N was found at its passive equilibrium length of 45 mm. This blocking force decreased to 0 N as a displacement of about 3 mm was reached. This displacement of 3 mm represented the maximum displacement of the actuator.

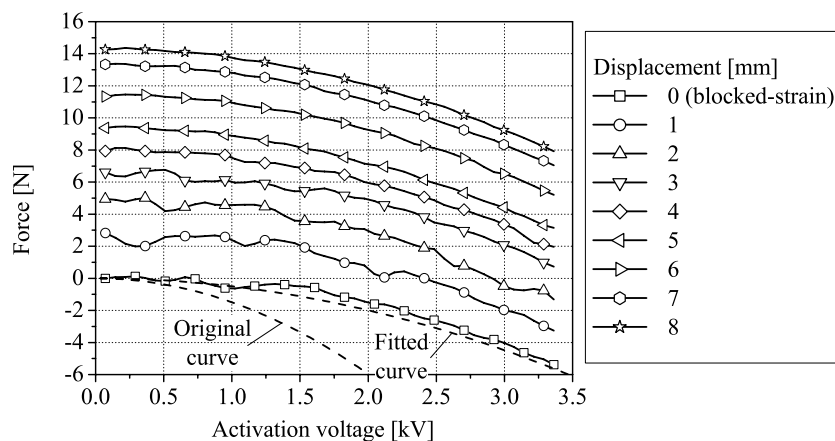


Figure 11. Force-voltage behavior of the actuator for given displacements.

We also observed that the blocking force decreased quadratically as the applied voltage was increased in Fig. 11. This observation corresponds to the theoretical considerations discussed in Sect. 3.2. The theoretical curves were plotted from Eqs. (5) by taking the actuator parameters in Tab. 2. The original curve strongly deviated from the experimental results. However, a well-fitted curve was achieved by correcting the original estimated forces with a factor of 1/3.

Table 2. Specifications of the spring roll DE actuators.

Name	Value
Material	VHB 4910 3M, thickness 1 mm
Dimensions	$\varnothing=12$ mm, $L=45$ mm
Layers	about 30-40
Weight	8 g
Activation voltage	3.5 kV
Max. blocking force	7.2 N
Max. stroke	5 mm
Manufacturing time	67 min
Active area	16×1840 mm ²
Pre-stretch factor	3×6.5
Relative permittivity	4.7
Diameter of the spring	7 mm

5. DEMONSTRATORS

As shown in Fig. 12, a prototype for a force feedback device was built. Three DE actuators were attached between the thumb and the index, the middle, and the ring finger via spherical joints. This system gives four DOF to each finger (flexion of the phalangeal joints, ab-/adduction of the metacarpophalangeal joint).

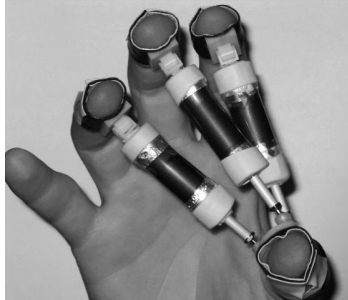


Figure 12. Prototype for the proposed force feedback concept with spring roll DE actuators.

6. CONCLUSIONS

In this paper, we presented a novel concept for a portable and kinematic-free force feedback device. Miniature spring roll DE actuators were manufactured and characterized. The considerations based on an incompressible material gave qualitative estimations of the blocking force under activation. The experimental results showed that the spring roll DE actuator can be potentially used in applications such as force feedback devices and robotics.

ACKNOWLEDGMENTS

This study has been funded by the Swiss National Science Foundation, and been greatly supported by Swiss Federal Laboratories for Materials Testing and Research (Empa). Particularly, we would like to thank Mr. Lukas Kessler, Claudio Iseli, and Urs Hintermüller for their support in actuator manufacturing, Mr. Alfred Schmidlin, Florentin Gröli for the actuator characterization and the prototype construction, and Mr. Philipp Boehringer for the device design.

REFERENCES

1. C. Youngblut, R. E. Johnson, S. H. Nash, R. A. Wienclaw, and C. A. Will, "Review of Virtual Environment Interface Technology," Tech. Rep. IDA Paper P-3186, Institute for Defense Analyses (IDA), 1801 N. Beauregard Street, Alexandria, Virginia 22311-1772, 1996. <http://www.hitl.washington.edu/scivw/IDA/>.
2. F. Hamit, *Virtual Reality and the Exploration of Cyberspace*, Sams Publishing, 1993.
3. www.immersion.com.
4. J. Gausemeier, J. Bauch, R. Radkowski, and Q. SHEN, "A Virtual Reality-based Design Environment for Self-Optimizing Mechatronic Systems," in *Mechatronics & Robotics '04*, P. Drews, ed., pp. 1333–1339, APS-European Center for Mechatronics, (Aachen), 13 - 15 Sept. 2004.
5. C. Spagno and A. Kunz, "Construction of a Three-sided Immersive Telecollaboration System," in *Proceeding of IEEE VR*, pp. 22–26, (Los Angeles, California), March 2003.
6. J. E. Atkins, R. A. Jacobs, and D. C. Knill, "Experience-dependent Visual Cue Recalibration based on Discrepancies between visual and Haptic Percepts," *Vision Research* **43**, pp. 2603–2613, 2003.
7. G. C. Burdea, *Force and touch feedback for virtual reality*, John Wiley & Sons, Inc., 1996.
8. www.sensible.com.
9. www.forcedimension.com.

10. F. Barbagli, K. Salisbury, and R. Devengenzo, "Enabling Multi-finger, Multi-hand Virtualized Grasping," in *Proceedings of IEEE International Conference of Robotics and Automation*, **1**, pp. 1259–1263, (Taipei), ICRA 2003.
11. P. Stergiopoulos, P. Fuchs, and C. Laugeau, "Design of a 2-Finger Hand Exoskeleton for VR Grasping Simulation," in *Eurohaptics*, (Dublin, Ireland), 2003.
12. M. Bouzit, G. Burdea, and G. e. a. Popescu, "The Rutgers Master II-New Design Force Feedback Glove," *IEEE/ASME Transactions on Mechatronics* **7**(2), pp. 256–263, 2002.
13. M. Bouzit, *Design, Implementation and Testing of a Data Glove with Force Feedback for Virtual and Real Objects Telematipulation*. Phd thesis, University of Pierre Et Marie Curie, 1996.
14. B. Choi and H. Choi, "SKK Hand Master-Hand Exoskeleton Driven by Ultrasonic Motors," in *Proceedings of the 2000 IEEE/RS International Conference on Intelligent Robots and Systems*, pp. 1131–1136, 2000.
15. A. Mazzone, R. Zhang, and A. Kunz, "Novel Actuators for Haptic Displays based on Electroactive Polymers," in *Virtual Reality Software and Technology Conference*, pp. 196–204, (Osaka Japan), 2003.
16. R. Zhang, A. Kunz, K. Gabor, M. Silvain, and A. Mazzone, "Dielectric Elastomer Actuators for A Portable Force Feedback Device," in *Proceedings of Eurohaptics 04*, pp. 300–307, (Muenchen, Germany), 2004.
17. R. Zhang, A. Kunz, P. Lochmatter, and G. Kovacs, "Dielectric Elastomer Spring Roll Actuators for a Portable Force Feedback Device," in *14th Symposium on Haptic Interfaces for Virtual Environment and Teleoperator systems, part of IEEE Virtual Reality 2006*, (Arlington, Washington D.C. U.S.A), 25-26 March 2006.
18. Q. Pei, R. Pelrine, S. Stanford, R. Kornbluh, and M. Rosenthal, "Electroelastomer rolls and their application for biomimetic walking robots," *Synthetic Metals* **135-136**, pp. 129–131, April 2003.
19. Q. Pei, M. Rosenthal, S. Stanford, H. Prahlad, and R. Pelrine, "Multiple-degrees-of-freedom electroelastomer roll actuators," *Smart Materials and Structures* **13**, pp. N86–N92, 2004.
20. D. Gomez, *A Dextrous Hand Master With Force Feedback For Virtual Reality*. Thesis, Electrical engineering, Rutgers-The State University of New Jersey, New Brunswick, 1997.
21. T. Brooks, "Telerobotic response requirements," in *Proc. IEEE Int. Conf. on Systems, man, and Cybernetics*, pp. 113–120, (Los Angeles, CA), 1990.
22. H. Tan, "Human factors for the design of force reflecting haptic interfaces," *Dynamic system and control* **DSC Vol. 55-1**(G0909A-1994), 1994.
23. R. Pelrine, P. Sommer-Larsen, R. Kornbluh, R. Heydt, G. Kofod, and Q. Pei, "Applications of Dielectric Elastomer Actuators," in *Proc. SPIE. Smart Structures and Materials 2001: Electroactive Polymer Actuators and Devices (EAPAD)*, **4329**, pp. 335–349, (Newport Beach, California USA), 2001.
24. F. Carpi, A. Migliore, G. Serra, and D. D. Rossi, "Helical dielectric elastomer actuators," *Smart Materials and Structures* **14**(6), pp. 1210–1216, 2005.
25. R. Ogden, "Large deformation isotropic elasticity - correlation of theory and experiment for compressible rubberlike solids," in *Proceedings of the Royal Society of London Series a-Mathematical and Physical Sciences*, **328(1575)**, p. 567, 1972.
26. R. Pelrine, R. Kornbluh, and J. Joseph, "Electrostriction of polymer dielectrics with compliant electrodes as a means of actuation," *Sensors and Actuators A: Physical* **64**(1), pp. 77–85, 1998.
27. *www.empa.ch*.